QRPA-based calculations for neutrino scattering and electroweak excitations of nuclei[*]

Arturo R. Samana[†]

[a]*Departamento de Ciências Exatas e Tecnológicas,*
Universidade Estadual de Santa Cruz,
Rodovia Jorge Amado km 16, 45650-000 Ilhéus-Ba, Brazil

Francisco Krmpotić, Alejandro E. Mariano, César A. Barbero
Departamento de Física, Facultad de Ciencias Exactas,
Universidad Nacional de La Plata, CP 1900 La Plata, Argentina and
Instituto de Física La Plata, CONICET,
115 y 49, CP 1900 La Plata, Argentina

Carlos A. Bertulani
Department of Physics, Texas A&M University Commerce,
P.O. Box 3011 Commerce, Texas 75429, USA

Nils Paar
Physics Department, Faculty of Science, University of Zagreb,
Bijenicka 32, HR-10002 Zagreb, Croatia

Abstract

A brief description of nuclear models used in the neutrino-nucleus reactions is performed, describing critically the general features, advantages and disadvantages. We focused on the neutrino-nucleus reactions at low energies due they present extremely subtle physical processes. They involve the weak interaction being very sensitive to the structure of nuclear ground states and excitations. The use of microscopic nuclear structure models in a consistent theoretical framework is therefore essential for a quantitative description of neutrino-nucleus reaction. These microscopic models include the nuclear shell model (SM), the random-phase approximation(RPA), continuum RPA (CRPA), hybrid models (CRPA+SM), quasiparticle RPA (QRPA), relativistic QRPA (RQRPA), and the Fermi gas model. The results with RPA- kind models to describe the nuclear matrix elements involved in neutrino-nucleus reactions, as such as electronic neutrino cross sections, muon capture rates and β^+ and β^- processes are compared. Some implications of QRPA based calculations with another weak processes, as such as the nuclear double beta decay ($\beta\beta$-decay), are also sketched.

INTRODUCTION

New types of nuclear weak processes have been measured in recent years as such as experimental works involving atmospheric, solar, reactor and accelerator neutrinos [1]. They are based on neutrino and antineutrino interactions with complex nuclei and, rather than being used to study the corresponding cross sections, they are mainly aimed to inquire on possible exotic properties of neutrino, which are not contained in the Standard Model of elementary particles. On the other size, converting an observed neutrino flux into a luminosity requires knowledge of the neutrino-nucleus cross sections for the detector material. In summary, the neutrino-nucleus cross section are strongly important to constrain the properties of neutrinos. In that direction, an accurate description of the nuclear structure of the nuclei involved in the weak interaction is fundamental. This issue demands a giant effort because the nuclear models to be used are dependent of the incident neutrino energy.

Some years ago, we marked the importance of the nuclear structure calculations on the analysis of neutrino oscillation in the LSND experiment [2]. The positive result of this experiment was confronted with the result of Karmen experiment [3], where no oscillation signal was presented. There are two LSND studies of the DIF $\nu_\mu \to \nu_e$ oscillations [1]. The first analysis was done on the 1993-1995 data sample [1], which gave a transition probability $P^{exp}_{\nu_\mu \to \nu_e} = (2.6 \pm 1.0 \pm 0.5) \times 10^{-3}$, when the cross-section σ_e predicted by Kolbe et al. within the CRPA is used [4]. The RPA-like models include high-lying one-particle one-hole excitations, but very frequently completely fail to account for the amount and distribution of the GT strength. This is the reason why the CRPA is unable to explain the weak processes (β-decays, μ-capture, and neutrino induced reactions) among the ground states of the triad $\{^{12}\text{B},^{12}\text{C},^{12}\text{N}\}$ [4]. Thus, it was interesting to reanalyze the LSND results in the framework of the projected QRPA (PQRPA) [2], which is the only RPA model that treats correctly the Pauli principle, explaining in this way the distribution of the GT strength, furnishing satisfactory results not only for the weak processes among the ground states of the triad $\{^{12}B, ^{12}C, ^{12}N\}$, but also for the inclusive weak processes [5]. The left-side of Figure 1 shows a comparison of the CRPA and PQRPA results for $\sigma_e(E_\nu), \sigma_e(E_\nu)\phi_\mu$ and $\sigma_e(E_\nu)\phi_\epsilon$, as a function of E_ν. The neutrino fluxes $\Phi_{\nu_\mu}, \Phi_{\nu_e}^{\pi^+}$ and $\Phi_{\nu_e}^{\mu^+}$ were adopted from the Ref. [1]. So, we have found that the employment of a smaller inclusive DIF $(\nu_e,^{12}\text{C})$ cross-section, than the one used by the LSND collaboration in the $\nu_\mu \to \nu_e$ oscillations study of the 1993-1995 data sample, leads to the following consequences: (i) the oscillation probability $P^{exp}_{\nu_\mu \to \nu_e}$ is increased, and (ii) the previously found consistence between the $(\sin^2 2\theta, \Delta m^2)$ confidence level regions for the $\nu_\mu \to \nu_e$ and the $\bar{\nu}_\mu \to \bar{\nu}_e$ oscillations is diminished. These effects are not due to the difference in the uncertainty ranges for the neutrino-nucleus cross-section, but to the difference in the cross-sections themselves.
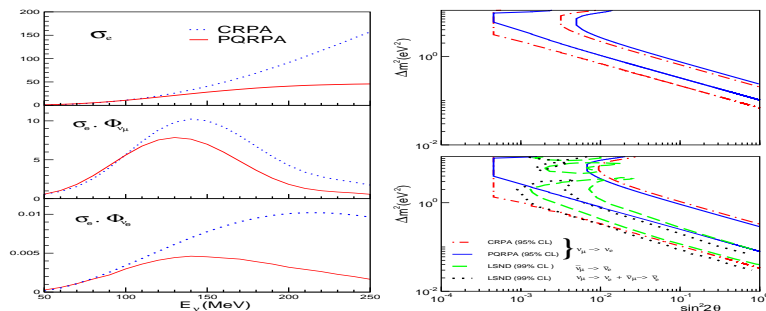
FIG. 1: Left-panel: Comparison between the CRPA and PQRPA results for: $\sigma_e(E_\nu)$ in units of 10^{-40} cm^2 (upper panel), and, in units of 10^{-52} POT $^{-1}$ MeV $^{-1}$, for $\sigma_e(E_\nu)\Phi_{\nu_\mu}$ (middle panel) and $\sigma_e(E_\nu)\Phi_{\nu_e}$ (lower panel). Right-panel: Regions in the neutrino oscillation parameter space. In the upper panel the results for $\nu_\mu \to \nu_e$ oscillations without the inclusion of the systematic uncertainty are shown, while the lower panel shows those with the uncertainty included [2].

The dynamics of supernova collapse and explosions as well as the synthesis of heavy nuclei are strongly dominated by neutrinos. For example, neutrinos carry away about 99% of gravitational binding energy in the core collapse of a massive star, and only a small fraction ($\sim 1\%$) is transferred to the stalled shock front, creating ejected neutrino fluxes observed in supernova remnants [6]. One important component of the detectors of supernovae neutrinos is ^{56}Fe. The KARMEN Collaboration measured (the only experimental data for a medium-heavy nucleus) the neutrino reaction ^{56}Fe(ν_e, e^-)^{56}Co from e^--bremsstrahlung with the detector surrounding shield [3]. This cross section is important to test the ability of nuclear models in explaining reactions on nuclei with masses around iron, which play an important role in supernova collapse. Experiments on neutrino oscillations such as MINOS [7] use iron as material detector, and future experiments , as such as SNS at ORNL [8]. The theoretical cross section was evaluated in several approximations as SM [9], Hybrid model SM+RPA [10] employed to estimate the number of events from ν-^{56}Fe reactions in the LVD detector [11], QRPA [12], relativistic QRPA (RQRPA) [13], and projected QRPA [14]. The ν_e-^{56}Fe cross sections were also described with the gross theory of beta decay (GTBD) [15], phenomenologically-based method of calculation which employs total muon capture rate data to determine the parameters necessary to calculate the inclusive neutrino cross sections [16], or using the local density approximation taking into account Pauli blocking, Fermi motion effects and renormalization of weak transition strengths in the nuclear medium [17].

WEAK-NUCLEAR INTERACTION FORMALISM

The most popular formalism for neutrino-nucleus scattering was developed by the Walecka group [18], where the nuclear transition matrix elements are classified as Coulomb, longitudinal, transverse electric, and transverse magnetic multipole moments related with the theoretical framework of previous electron scattering [19]. We feel that these denominations might be convenient when discussing simultaneously charge-conserving, and charge-exchange processes, but seems unnatural when one considers only the last ones. On the other hand, this terminology is not often used in nuclear β-decay and μ-capture, where one only speaks of vector and axial matrix elements with different degrees of forbiddenness: allowed (GT and Fermi), first forbidden, second forbidden, etc., types. Motivated by this fact, our group developed a proper formalism of weak interaction [5], obtaining new expressions for the transition rates. When studying neutrino induced reactions
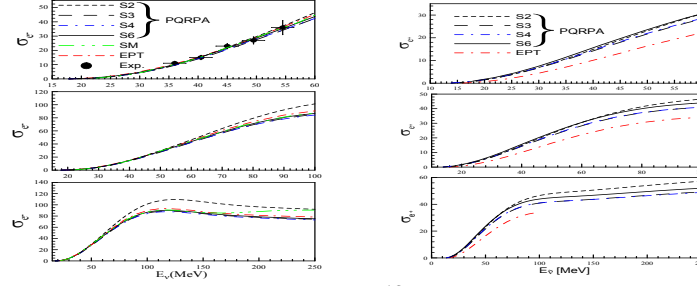
FIG. 2: Left-panel: Comparison of exclusive neutrino-^{12}C cross sections (in units of 10^{-42} cm^2) evaluated in the PQRPA model [27], the SM [40], and EPT [37] calculations. The experimental data in the DAR region are from Ref. [1]. Right-panel: Similar comparison of nuclear model results for ^{12}C$(\tilde{\nu}, e^+)^{12}$B cross-sections. [27].

[20, 21] it is sometimes preferred to employ the formulation done by Kuramoto *et al.*[22], mainly because of its simplicity. But, the latter formalism does not include the velocity dependent terms in the hadronic current and it does not include the muon capture rates. Therefore, To describe simultaneously the neutrino-nucleus reactions and μ-capture processes it is necessary to resort to additional theoretical developments, such as those of Luyten *et al.* [23] and Auerbach and Klein [24].

In all the cases, the weak Hamiltonian is expressed in the form [18, 25, 26] $H_W(\mathbf{r}) = \frac{G}{\sqrt{2}} J_\alpha l_\alpha e^{-i\mathbf{r}\cdot\mathbf{k}}$, where $G = (3.04545 \pm 0.00006)\times 10^{-12}$ is the Fermi coupling constant (in natural units), the leptonic current $l_\alpha \equiv \{\mathbf{l}, il_\emptyset\}$ is given by the Eq. (2.3) in Ref. [5] and the hadronic current operator $J_\alpha \equiv \{\mathbf{J}, iJ_\emptyset\}$ in its nonrelativistic form reads

$$J_\emptyset = g_{\rm V} + (\overline{g}_{\rm A} + \overline{g}_{\rm P1})\boldsymbol{\sigma}\cdot\hat{\mathbf{k}} + g_A \frac{i\boldsymbol{\sigma}\cdot\boldsymbol{\nabla}}{\rm M}, \tag{1}$$

$$\mathbf{J} = -g_{\rm A}\boldsymbol{\sigma} - i\overline{g}_{\rm W}\boldsymbol{\sigma}\times\hat{\mathbf{k}} - \overline{g}_{\rm V}\hat{\mathbf{k}} + \overline{g}_{\rm P2}(\boldsymbol{\sigma}\cdot\hat{\mathbf{k}})\hat{\mathbf{k}} - g_{\rm V}\frac{i\boldsymbol{\nabla}}{\rm M},$$

where $\hat{\mathbf{k}} \equiv \mathbf{k}/|\mathbf{k}|$. The quantity $k = P_i - P_f \equiv \{\mathbf{k}, ik_\emptyset\}$ is the momentum transfer, M is the nucleon mass, and P_i and P_f are momenta of the initial and final nucleon (nucleus). The effective vector, axial-vector, weak-magnetism and pseudoscalar dimensionless coupling constants are, respectively $g_V = 1$, $g_A = 1$, $g_M = \kappa_p - \kappa_n = 3.70$, $g_P = g_A \frac{2Mm_\ell}{k^2+m_\pi^2}$, where the auxiliary coupling constant $\overline{g}_{\rm V}, \overline{g}_{\rm A}, \overline{g}_{\rm W}, \overline{g}_{\rm P1}, \overline{g}_{\rm P2}$ are defined in [5]. The conserved vector current (CVC) hypothesis, and the partially conserved axial vector current (PCAC) hypothesis are assumed. The finite nuclear size (FNS) effect is incorporated via the dipole form factor with a cutoff $\Lambda = 850$ MeV, i.e., $g \to g \left[\Lambda^2/(\Lambda^2 + k^2)\right]^2$.

In performing the multipole expansion of the nuclear operators it is convenient 1) to take the momentum $\mathbf{k}$ along the z axis using the spherical Bessel-Fourier series for $e^{-i\mathbf{k}\cdot\mathbf{r}}$, and 2) to define the operators O_α as

$$\mathsf{O}_{\emptyset\mathsf{J}} = j_\mathsf{J}(\rho)Y_{\mathsf{J}0}(\hat{\mathbf{r}})J_\emptyset \equiv g_v \mathcal{M}_\mathsf{J}^V + ig_A \mathcal{M}_\mathsf{J}^A + i(\overline{g}_{\rm A} + \overline{g}_{\rm P1})\mathcal{M}_{0\mathsf{J}}^A, \tag{2}$$

$$\mathsf{O}_{m\mathsf{J}} = \sum_\mathsf{L} i^{\mathsf{J}-\mathsf{L}} F_{\mathsf{L}\mathsf{J}m} j_\mathsf{L}(\rho) \left[Y_\mathsf{L}(\hat{\mathbf{r}}) \otimes \mathbf{J}\right]_\mathsf{J} \equiv i(\delta_{m0}\overline{g}_{\rm P2} - g_{\rm A} + m\overline{g}_{\rm W})\mathcal{M}_{m\mathsf{J}}^A + g_v \mathcal{M}_{m\mathsf{J}}^V - \delta_{m0}\overline{g}_{\rm V}\mathcal{M}_\mathsf{J}^V,$$

where $F_{\mathsf{L}\mathsf{J}m} = (-)^{1+m}(1, -m\mathsf{J}m|\mathsf{L}0)$, is a Clebsch-Gordan coefficient defined in Ref. [27]. The elementary operators are given by

$$\mathcal{M}_\mathsf{J}^V = j_\mathsf{J}(\rho)Y_\mathsf{J}(\hat{\mathbf{r}}) \ , \ \mathcal{M}_\mathsf{J}^A = {\rm M}^{-1}j_\mathsf{J}(\rho)Y_\mathsf{J}(\hat{\mathbf{r}})(\boldsymbol{\sigma}\cdot\boldsymbol{\nabla}), \tag{3}$$

$$\mathcal{M}_{m\mathsf{J}}^A = \sum_{\mathsf{L}\geq 0} i^{\mathsf{J}-\mathsf{L}-1} F_{\mathsf{L}\mathsf{J}m} j_\mathsf{L}(\rho) \left[Y_\mathsf{L}(\hat{\mathbf{r}}) \otimes \boldsymbol{\sigma}\right]_\mathsf{J} \ , \ \mathcal{M}_{m\mathsf{J}}^V = {\rm M}^{-1}\sum_{\mathsf{L}\geq 0} i^{\mathsf{J}-\mathsf{L}-1} F_{\mathsf{L}\mathsf{J}m} j_\mathsf{L}(\rho)[Y_\mathsf{L}(\hat{\mathbf{r}}) \otimes \boldsymbol{\nabla}]_\mathsf{J}.$$
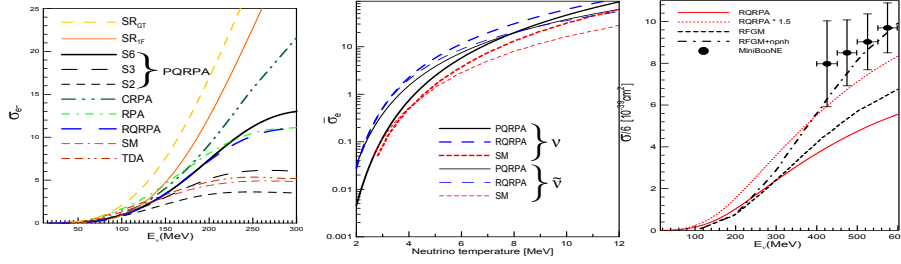
FIG. 3: Left-panel: Inclusive ^{12}C$(\nu,e^-)^{12}$N cross-section $\sigma_{e^-}(E_\nu)$(in units of 10^{-39} cm^2) plotted as a function of the incident neutrino energy E_ν for PQRPA [27], RPA [21], CRPA [10], and RQRPA within S_{20} for E_{2qp}=100 MeV [13], SM [21], TDA [18] and global calculations SR_{GT}, and SR_{1F}. Central-panel: Flux-averaged neutrino and antineutrino cross sections $\overline{\sigma}_{e\pm}$ in ^{12}C with typical supernovae fluxes [27]. Right-panel:RQRPA cross section per neutron (full line) [27] compared with that for the $(\nu_\mu,^{12}$C$)$ scattering data measured at MiniBooNE [35], with dotted line is shown the same calculation but renormalized by a factor 1.5, RFGM for pure (1p-1h) excitations (dashed line), and with the inclusion of the np-nh channels (dot-dashed line) [33, 41].

The comparison with the Walecka's formalism-[18] was established in the equation (A.11) of Ref. [27], and where the seven nuclear matrix elements, denoted as: $M_J^M, \Delta_J^M, \Delta'^M_J, \Sigma_J^M, \Sigma'^M_J, \Sigma''^M_J$ and Ω_J^M, are also the elementary operators defined in Equation (3).

The transition amplitude for the neutrino-nucleus reaction at a fixed value of κ, from the initial state $|0^+\rangle$ in the (Z,N) nucleus to the n-th final state $|J_n^\pi\rangle$ in the nucleus $(Z \pm 1, N \mp 1)$, reads $\mathcal{T}_{J_n^\pi}(\kappa) \equiv \sum_{s_\ell,s_\nu} |\langle J_n^\pi|H_W(\kappa)|0^+\rangle|^2$. The momentum transfer here is $k = p_\ell - q_\nu$, with $p_\ell \equiv \{\mathbf{p}_\ell, iE_\ell\}$ and $q_\nu \equiv \{\mathbf{q}_\nu, iE_\nu\}$, and after some algebra [5] one gets

$$\mathcal{T}_{J_n^\pi}(\kappa) = 4\pi G^2 [\sum_{\alpha=\emptyset,0,\pm 1} |\langle J_n^\pi||\mathsf{O}_{\alpha \mathsf{J}}(\kappa)||0^+\rangle|^2 \mathcal{L}_\alpha - 2\Re \left(\langle J_n^\pi||\mathsf{O}_{\emptyset \mathsf{J}}(\kappa)||0^+\rangle \langle J_n^\pi||\mathsf{O}_{0 \mathsf{J}}(\kappa)||0^+\rangle^*\right) \mathcal{L}_{\emptyset 0}], \quad (4)$$

where $\mathcal{L}_\emptyset, \mathcal{L}_0, \mathcal{L}_{\pm 1}, \mathcal{L}_{\emptyset 0}$ are the lepton traces, with $\theta \equiv \hat{\mathbf{q}}_\nu \cdot \hat{\mathbf{p}}_\ell$ being the angle between the incident neutrino and ejected lepton momenta, defined in [27].

The exclusive cross-section (ECS) for the state $|J_n^\pi\rangle$, as a function of the incident neutrino energy E_ν, is

$$\sigma_\ell(J_n^\pi, E_\nu) \;=\; \frac{|\mathbf{p}_\ell|E_\ell}{2\pi} F(Z+S, E_\ell) \int_{-1}^{1} d(\cos\theta) \mathcal{T}_{J_n^\pi}(\kappa), \quad (5)$$

where E_ℓ is the electron energy, and $\omega_{J_n^\pi} = -k_\emptyset = E_\nu - E_\ell$ is the excitation energy of the state $|J_n^\pi\rangle$ relative to the state $|0^+\rangle$. Moreover, $F(Z+S, E_\ell)$ is the Fermi function for neutrino ($S = 1$), and antineutrino ($S = -1$), respectively. The inclusive cross-section (ICS) reads, $\sigma_\ell(E_\nu) = \sum_{J_n^\pi} \sigma_\ell(J_n^\pi, E_\nu)$, as well as with folded cross-sections, both exclusive,

$$\overline{\sigma}_\ell(J_n^\pi) = \int dE_\nu \sigma_\ell(J_n^\pi, E_\nu)\Phi_\ell(E_\nu) \;\;,\;\; \overline{\sigma}_\ell = \int dE_\nu \sigma_\ell(E_\nu)\Phi_\ell(E_\nu), \quad (6)$$

and inclusive, respectively, where $\Phi_\ell(E_\nu)$ is the neutrino (antineutrino) normalized flux.

ON NUCLEAR MODELS AND WEAK PROCESSES CALCULATIONS

In a general way, the theoretical models can be divided generically into: (i) models with micro-scopical formalism with a detailed nuclear structure, solving the microscopic quantum-mechanical Schrodinger or Dirac equation, provides nuclear wave functions and g.s.-shape E_{sp} , J^π nuclear

spin , log (ft) value, $\tau_{1/2}$ half-life, etc, i.e., Shell Model [28] and RPA-like models as self-consistent Skyrme-HFB+QRPA [29], quasiparticle RPA (QRPA), projected QRPA[30], relativistic QRPA (RQRPA) [31], and density Functional+Finite Fermi System [32]; (ii) models describing overall nuclear properties statistically where the parameters are adjusted to experimental data trough polynomial or algebraic express and there is no a nuclear wave function, for example, Fermi Gas -based Model [33] and Gross Theory of β-decay (GTBD) [34]. It is a difficult task to have one nuclear model that takes into account all the incident neutrinos energy. Several experiments with different sources of neutrinos can adopt one or another model to simulate the neutrino interaction via Monte Carlo and after to measure it in the experiment. For example, present atmospheric and accelerator-based neutrino oscillation experiments involve ^{12}C and operate at neutrino energies $E_\nu \sim 1$ GeV to access the relevant regions of the oscillation parameter space. This is the case of the MiniBooNE detector [35], which uses the light mineral oil containing the CH2 molecule. Another interval of energy is employed when supernovae neutrinos are studied. The corresponding neutrinos, which carry all flavors were observed in only one occasion (SN1987A), have an energy $E_\nu \lesssim 100$ MeV [36]. For the planned experimental searches of supernovae neutrino signals, which involve ^{12}C as scintillator liquid detector, the precise knowledge of neutrino cross sections of ^{12}N and ^{12}B ground-states (with energies of the order of 10 MeV), *i.e.*, of $\sigma_{e^-}(E_\nu, 1_1^+)$, and $\sigma_{e^+}(E_{\tilde\nu}, 1_1^+)$ is very important. In fact, in the LVD experiment [11] the number of events detected during the supernova explosion are estimated by convoluting the neutrino supernova flux with: (i) the inter-action cross sections, (ii) the efficiency of the detector, and (iii) the number of target nuclei. For the carbon content of the LVD detector have been used so far $\sigma_{e^-}(E_\nu, 1_1^+)$, and $\sigma_{e^+}(E_{\tilde\nu}, 1_1^+)$, as obtained from the Elementary Particle Treatment (EPT) [37].

So then, we can adopt in low energy region (up to 100 MeV) some accurate shell model (SM) description or RPA-like models and also depending if we are interested to describe exclusive or inclusive quantities. In particular the RPA-like models are by far simpler computationally than the SM. Note that the kind of correlations that these two methods include are not the same. For example, the QRPA makes a large fraction of nucleons to take part in within a large single-particle space, but within a modest configuration space. The shell model, by contrast, deals with a small fraction of the nucleons in a limited single-particle space, but allows them to correlate in arbitrary ways within a large configuration space [38]. It is clear that the nuclear structure descriptions inspired on the Relativistic Fermi Gas Model (RFGM) [39], which do not involve multipole expansions, should only be used for inclusive quantities. A brief report of the nuclear models employed for ^{12}C is presented in Ref.[27].

Now, we describe some results obtained in ^{12}C and ^{56}Fe, nuclei that are using in current neutrino oscillation experiments, and some topics on double beta decay calculations. The PQRPA calculations [5] solved the puzzle found for Volpe et al. [21] related to the collectivity on the ground state in ^{12}C. In Ref. [27] were studied neutrino and antineutrino charge-exchange reactions on 12C using the PQRPA and RQRPA in different configuration spaces to analyze their dependence on the configuration space. Figure 2 shows the exclusive ^{12}C$(\nu, e^-)^{12}$N cross-section $\sigma_e(E_\nu, 1_1^+)$, plotted as a function of the incident neutrino energy E_ν. Results for several single-particle spaces S_N , and $t = 0$ for S_2, and S_3, $t = 0.2$ for S_4, and $t = 0.3$ for S_6, within three different energy intervals, are shown. The SM, and EPT calculations are, respectively, from Refs. [40], and [37]. The experimental data in the DAR region are from Ref. [1]. In similar way, the right-panel of Figure 2 shows the calculated $(\tilde\nu, ^{12}$C$)$ cross-section $\sigma_{e^+}(E_{\tilde\nu}, 1_1^+)$, plotted as a function of the incident antineutrino energy $E_{\tilde\nu}$ in the same parametrization spaces.

The left-panel of Figure 3 shows the inclusive ^{12}C$(\nu, e^-)^{12}$N cross-section $\sigma_{e^-}(E_\nu)$ plotted as a function of the incident neutrino energy E_ν. The PQRPA results within the s.p. spaces S_2, S_3, and S_6, and the same values of $s = t$ [57]. These are compared with two sum rule limits (global calculations): SR_{GT}, and SR_{1F} obtained with average excitation energy $\overline{\omega_{J_n^\pi}}$ of 17.34, and 42 MeV,
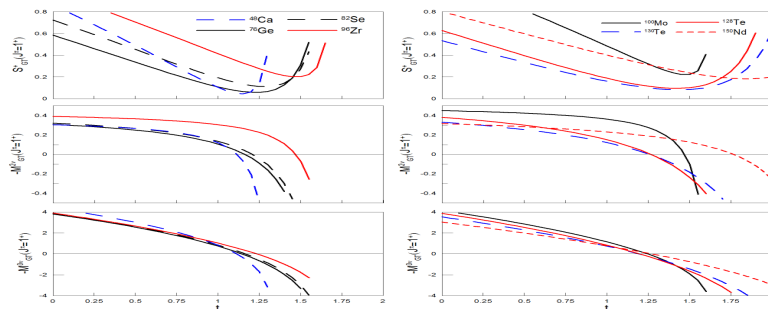
FIG. 4: S_{GT}^+, $M_{GT}^{2\nu}$, e $M_{GT}^{0\nu}$ as a function of the parameter particle-particle t evaluated in the QRPA [51]

respectively. Several previous RPA-like calculations, namely: RPA [21], CRPA [10], and RQRPA within S_{20} for E_{2qp}=100 MeV [13], as well as the SM [21], and the TDA [18] are also shown. The central-panel of Figure 3 shows the flux-averaged neutrino and antineutrino cross sections $\overline{\sigma}_{e\pm}$ in ^{12}C with typical supernovae fluxes showing that in the interval of temperatures $T_\nu = 3-5$ MeV: (i) σ for antineutrinos is going larger to similar of σ for neutrinos and, (ii) the results obtained with SM are always smaller than PQRPA and RQRPA calculations [27]. Finally, in the right-panel of Figure 3 shows the calculated RQRPA (within S_{30} and $E_{2qp} = 500$ MeV) quasi-elastic $(\nu_e, ^{12}$C) cross section per neutron (full line) when is compared with that for the $(\nu_\mu, ^{12}$C) scattering data measured at MiniBooNE [35]; with dotted line is shown the same calculation but renormalized by a factor 1.5. Also are displayed the calculations done by Martini *et al.* [33, 41] within the RFGM+RPA for pure (1p-1h) excitations (dashed line), and with the inclusion of the np-nh channels (dot-dashed line).

In Ref. [14] were evaluated the inclusive ^{56}Fe$(\nu_e, e^-)^{56}$Co cross sections evaluated in QRPA and PQRPA, in the DAR region. They were compared with those obtained with other nuclear structure models: GTBD [15], Hybrid [42], QRPA$_S$ [12], and RQRPA [13]. Table 1 in Ref.[14] shown the comparison of these folded cross section, where all the theoretical models agree with the experimental value due the experimental error in the measured value. The number of events detected for supernova is calculated as,

$$N_\alpha = N_t \int_0^\infty \Phi_\alpha(E_\nu) \cdot \sigma(E_\nu) \cdot \epsilon(E_\nu) dE_\nu, \tag{7}$$

where the index $\alpha = \nu_e, \bar{\nu}_e, \nu_x$ and $(\nu_x = \nu_\tau, \nu_\mu, \bar{\nu}_\mu, \bar{\nu}_\tau)$ indicates the neutrino or antineutrino type, N_t is the number of target nuclei, $\Phi_\alpha(E_\nu)$ is the neutrino flux, $\sigma(E_\nu)$ is the neutrino-nucleus cross section, $\epsilon(E_\nu)$ is the detection efficiency, and E_ν is the neutrino energy. Recent calculations by the LVD group [11] estimate that the $(\nu_e + \bar{\nu}_e)$ interactions on ^{56}Fe are almost 17% of the total detected signal. The time-spectra can be approximated by the zero-pinched Fermi-Dirac distribution. For the reactions $(\nu_e, ^{56}$Fe$)$, Ref.[14] calculated N_e and $\tilde{N}_e$ as a function of the neutrino temperatures T_{ν_e} and T_{ν_x}, folding $\sigma_e(E_\nu)$ from different nuclear structure models with the neutrino fluxes $\Phi^0_{\nu_e}(E_\nu, T_{\nu_e})$ and $\Phi^0_{\nu_x}(E_\nu, T_{\nu_x})$, respectively.

We have marked the importance of the semileptonic weak interaction processes in nuclei are very sensitive to detailed properties of nuclear ground states and excitations [43]. Marketin *et al.* [44] performed systematics calculations on muon capture rates for nuclei with $6 \leq Z \leq 94$ using RQRPA. Another RPA systematics calculations were performed by Zinner *et al.*[45]. On the other hand, we have shown that, when the capture of muons is evaluated in the context of the PQRPA, the conservation of the number of particles is very important not only for carbon but in all light nuclei with $A \leq 30$. The consequence of this is the superiority of the PQRPA on the QRPA in this nuclear mass region, where systematic calculations of muon capture rates with these models were performed [46]. One step beyond is made with RQRPA calculations to provide

a self-consistent microscopic description of neutrino-nucleus cross sections involving a large pool of $Z = 8 - 82$ nuclei for the implementation in models of nucleosynthesis and neutrino detector simulations. They performed a large-scale calculations of charged-current neutrino-nucleus cross sections, including those averaged over supernova neutrino fluxes, for the set of even-even target nuclei from oxygen toward lead ($Z = 8 - 82$), spanning $N = 8 - 182$ (O-Pb pool) [47].

We do not until this moment which is the absolute scale mass, and whether the neutrino is a Majorana or Dirac particle. The atomic nuclei are the detectors of the evasive neutrinos and the key of this puzzle is the neutrinoless double beta decay. The three commonly $\beta\beta$-decay processes are: (i) the two-neutrino $\beta\beta$-decay ($2\nu\beta\beta$); (ii) the neutrinoless $\beta\beta$-decay ($0\nu\beta\beta$) and; (iii) the neutrinoless $\beta\beta$-decay with majoron emission ($0\nu\chi\beta\beta$). The inverse half-life for the $0^+ \to 0^+$ and nuclear matrix elements (NME's) are related as [38, 48]:

$$T_{1/2}^{-1} = \mathcal{G}(\mathcal{MF})^2 \ , \qquad \mathcal{F} = \begin{cases} 1 & , \text{for} \quad 2\nu\beta\beta \\ \langle m_\nu \rangle / m_e; & , \text{for} \quad 0\nu\beta\beta \\ \langle g_M \rangle; & , \text{for} \quad 0\nu\chi\beta\beta \end{cases} , \qquad (8)$$

where $\mathcal{G}$ is a kinematical factor which depends on the corresponding phase space, $\mathcal{M}$ is the NME and the values in $\mathcal{F}$ are $\langle m_\nu \rangle$ and $\langle g_M \rangle$ respectively the effective neutrino masses and the effective majoron-neutrino coupling. $\mathcal{M}_{2\nu}$ and $\mathcal{M}_{0\nu}$ present many similar features and it can be established that we shall not understand the $0\nu\beta\beta$-decay unless we understand the $2\nu\beta\beta$-decay. In other words, if we found an agreement between experimental and theoretical values for $\mathcal{M}_{2\nu}$, it is possible used the same nuclear model (and parametrization) to describe consistently $\mathcal{M}_{0\nu}$. There is an extensive literature on the theoretical estimations of NME of double beta decay using the QRPA model [49, 50]. In a recent work [50], the authors claim to achieve partial restoration of the isospin symmetry and hence fulfillment of the requirement that the $2\nu\beta\beta$ Fermi matrix element $M_F^{2\nu}$ vanishes. But this procedure was used previously in the pioneer work of Krmpotić and S. Sharma [48]. Using that receipt, we reproduce the single GT-β^+ strength (S_{GT}^+), NME for Gamow-Teller of $2\nu\beta\beta$ ($M_{GT}^{2\nu}$), and NME for Gamow-Teller of $0\nu\beta\beta$ ($M_{GT}^{0\nu}$), as a function of the particle-particle parameter t in the residual interaction are shown in Figure 4. These results were obtained using a numerical code that summarizes and gives a new fashion of the formalism presented in Refs. [49] for the $2\nu\beta\beta$ and $0\nu\beta\beta$, based on the Fourier-Bessel expansion of the weak Hamiltonian, adapted for nuclear structure calculations [51].

Another kind RPA formalism for $2\nu\beta\beta$ was proposed some years ago based on the Four Quasiparticle Tamm-Dancoff Approximation (FQTDA). Several serious inconveniences found in the QRPA are not present in the FQTDA, such as the ambiguity in treating the intermediary states, and further approximations necessary for evaluation of the nuclear matrix elements or, the extreme sensitivity of NME with the ratio between the pn and pp + nn pairings [38]. Some improvements on this model and their extension to open shell nuclei is being studied [52].

SUMMARY

A brief description of nuclear models used in the neutrino-nucleus reactions was performed, describing critically the general features, advantages and disadvantages. We focused on the neutrino-nucleus reactions at low energies due they present extremely subtle physical processes.

We noted that all the formalism to describe weak-nuclear interaction present in the literature are equivalents. Some of the most used formalism were developed by: (i) O'Connell, Donelly & Walecka [18], where seven irreducible tensor operators (ITO) are obtained and they compose the nuclear matrix elements called by longitudinal, Coulomb, transversal electric, transversal magnetic according to those found in electron scattering formalism [19]; (ii) Kuramoto *et al.*. [22], where the

nuclear hamiltonian is expanded up to $(|k|/M)^3$, where $|k|$ is the momentum transfer and M is the mass of nucleon; (iii) Luyten *et al.*. [23], developed to evaluate muon capture rates, (iv) Krmpotić *et al.*. [5], this uses a notation more familiar to the nuclear β-decay, where one works with allowed, first forbidden, second forbidden, etc transitions.

The microscopic RPA-like models, as such as the QRPA, are extensively used to evaluate weak-nuclear observables. They have some disadvantages, *i.e.,* to work with low energy neutrino regions up to 250 MeV; many of these QRPA are using the Skyrme interaction as residual interaction, but is not good enough to make decisive improvement, and the Gogny interaction is employed to check the Skyrme results; developed essentially for spherical nuclei, and there is a few QRPA model to non-spherical nuclei [53]. The advantages are: a self-consistent treatment, lead to large spaces, excellent agreement with exclusive reaction as well as the SM, with a well description of inclusive reaction and, it is possible to describe reaction up to 600 MeV neutrino energy with relativistic QRPA; a good option for astrophysical systematic calculations and; QRPA is the main tool for double beta decay in the last 30 years. Some improvements are planned through the Universal Nuclear Density Functional - UNEDF [54], and the extension to non-spherical nuclei. The SM is the other microscopical model most widely used. This model has the next disadvantages: only works with magic nuclei ($N = 50, 82, 126$) due they need a great computational effort to open the shells, only treats GT-decay and; to avoid a great computational task, some cut-offs due to configurational space are imposed that could be dangerous violating some sum rules. The advantages of this model is that several essential correlations are included, leading to a correct treatment of even-even and odd isotopes. Some improvements are coming from the ab-initio shell model, where new advances are obtained in nuclei as ^{12}C and ^{16}O [55], ^{48}Ca and ^{124}Sn [56].

Some results with RPA-kind models to describe the nuclear matrix elements involved in neutrino-nucleus reactions were compared. Some implications of QRPA based calculations with another weak processes, as such as the nuclear double beta decay ($\beta\beta$-decay), were also sketched.

———————

† `arsamana@uesc.br`; Speaker

[1] A. Aguilar *et al.* [LSND collaboration], Phys. Rev. D **64**, 112007 (2001), and references therein.

[2] A. Samana *et al.* , Phys. Lett. **B642**, 100 (2006).

[3] KARMEN Collaboration, R. Maschuw, $http://www-ik1.fzk.de/karmen/cc-e.html/article$

[4] E. Kolbe *et al.* , Phys. Rev. C **49**, 1122 (1994); E. Kolbe *et al.* Nucl. Phys. **A652** (1999) 91.

[5] F. Krmpotić *et al.*Phys. Rev. C **71**, 044319 (2005).

[6] H. Duan *et al.* , Phys. Rev. D 74, 105014 (2006).

[7] MINOS Collaboration, P. Adamson *et al.*, Phys. Rev. D **76**, 072005 (2007).

[8] Y. Efremenko, Nucl. Phys. **B138**(Proc. Suppl), 343 (2005)

[9] E.V. Bugaev *et al.* , Nucl. Phys. **A324**, 350 (1979).

[10] E. Kolbe *et al.* , Phys. Rev. C **60**, 052801 (1999); E. Kolbe *et al.*, Nucl. Phys. **A652**, 91 (1999).

[11] N.Yu. Agafonova *et al.*, Astron. Phys. **27**, 254 (2007).

[12] R. Lazauskas and C. Volpe, Nucl. Phys. **A792**, 219 2007).

[13] N. Paar *et al.* , Phys. Rev. C **77**, 024608 (2008).

[14] A.R. Samana and C.A. Bertulani, Phys. Rev. C **78**, 024312 (2008)

[15] N. Itoh and Y. Kohyama, Nucl. Phys. **A306**, 527 (1978).

[16] S. Mintz, J. Phys. G **28**, 451 (2002).

[17] M.S. Athar *et al.* , Nucl. Phys. **A764**, 551 (2006).

[18] J.D. Walecka, *Theoretical Nuclear and Subnuclear Physics* (Oxford University Press, New York, 1995) p. 531, and references therein.

[19] T. de Forest and J.D. Walecka, Adv. in Phys. **15** (1966) 1

[20] N. Auerbach *et al.*, Phys. Rev. C **56**, R2368 (1997).

[21] C. Volpe *et al.* , Phys. Rev. C **62**, 015501 (2000).

[22] T. Kuramoto *et al.*, Nucl. Phys. **A512**, 711 (1990).

[23] J. R. Luyten *et al.*, H. P. C. Rood, and H. A. Tolhoek, , Nucl. Phys. **41**, 236 (1963).

[24] N. Auerbach and A. Klein, Nucl. Phys. **A395**, 77 (1983).

[25] T.W. Donnelly and R. D. Peccei, Phys. Rep. **50**, 1 (1979).

[26] R.J. Blin-Stoyle and S.C.K. Nair, Advances in Physics **15**, 493 (1966).

[27] A. R. Samana *et al.*, Phys. Rev. C **83**, 023403 (2011).

[28] Martinez *et al.*, Phys. Rev. Lett. **83** (1999) 4502.

[29] J. Engel *et al.* , Rev. C **60**, 14302 (1999).

[30] F. Krmpotić *et al.*, Phys. Lett. **B319**, 393 (1993).

[31] N. Paar *et al.*,Phys. Rev. C **69**, 054303 (2004).

[32] I. N. Borzov and S. Goriely, Phys. Rev. C **62** (2000) 035501.

[33] M. Martini *et al.* , Phys. Rev. C **80**, 065501 (2009).

[34] K. Takahashi and M. Yamada, Prog. Theor. Phys. **41**, 1470 (1969).

[35] A. A. Aguilar-Arevalo *et al.*(MiniBooNE Collaboration), Nucl. Instrum. Methods A **599**, 28 (2009).

[36] A. Strumia and F. Vissani, arXiv: hep-ph/0606054v2.

[37] M. Fukugita *et al.*, Phys. Lett. **B12**, 139 (1988).

[38] F. Krmpotić, Fizika **B14**, 139 (2005).

[39] M. Valverde *et al.* , Phys. Lett. B 638, 325 (2006).

[40] J. Engel *et al.* , Phys. Rev. C **54**, 2740 (1996).

[41] M. Martini *et al.* , Phys. Rev. C **81**, 045502 (2010).

[42] E. Kolbe and K. Langanke, Phys. Rev. C **63**, 025802 (2001).

[43] A. R. Samana *et al.* , New Journal of Physics **10**, 033007 (2008).

[44] T. Marketin *et al.*, Phys. Rev. C **79**, 054323 (2009).

[45] N.T. Zinner *et al.*, Phys. Rev. C **74**, 024326 (2006).

[46] D. Sande Santos *et al.* , Proceedings of Science, http://pos.sissa.it/archive/conferences/142/120/ XXXIV%20BWNP_120.pdf

[47] N. Paar *et al.* , Phys. Rev. C **87**, 025801 (2013); N. Paar *et al.* , arXiv:1505.07486 [nucl-th].

[48] F Krmpotić and S. Shelly Sharma, Nucl. Phys. **A572**, 329 (1994), and references therein.

[49] C. Barbero *et al.*, Nucl. Phys. **A650** (1999) 485, and references therein.

[50] F. Simkovic *et al.* , Phys. Rev. C **87**, 045501 (2013).

[51] C. A. Barbero *et al.* AIP Conference Proceedings **1625**, 169 (2014).

[52] L. de Oliveira *et al.* , Journal of Physics: Conference Series **630** (2015) 012048

[53] R. Alvarez-Rodriguez *et al.*, Phys. Rev. C **70**, 064309 (2004)

[54] UNEDF SciDAC Collaboration, http://www.unedf.org/

[55] James P. Vary *et al.*, arXiv:1507.04693 [nucl-th].

[56] R.A. Senkov, M. Horoi. Phys. Rev. C **88**, 064312 (2013).

[57] s is the particle-particle strength parameter for singlet channel, and t is the particle-particle strength parameter for triplet channel for the residual δ-interaction [27].